frontiers | Frontiers in Earth Science

REVIEW
published: 19 May 2022
doi: 10.3389/feart.2022.868701

Dispersion of Benthic Plumes in Deep-Sea Mining: What Lessons Can Be Learned From Dredging?

Rudy Helmons[1,2]*, *Lynyrd de Wit*[3], *Henko de Stigter*[4] and *Jeremy Spearman*[5]

[1]Technische Universiteit Delft, Offshore and Dredging Engineering, Delft, Netherlands, [2]Norwegian University of Science and Technology, Mineral Production and HSE, Trondheim, Norway, [3]Stichting Deltares, Ecosystems and Sediment Dynamics, Delft, Netherlands, [4]Royal Netherlands Institute for Sea Research, Texel, Netherlands, [5]HR Wallingford, Dredging and Coasts & Oceans, Wallingford, United Kingdom

Over the past decade, deep-sea mining (DSM) has received renewed interest due to scarcity of raw materials. Deep-sea mining has been spurred by the need for critical resources to support growing populations, urbanization, high-tech applications and the development of a green energy economy. Nevertheless, an improved understanding of how mining activities will affect the deep-sea environment is required to obtain more accurate assessment of the potential environmental impact. In that regard, the sediment plumes that are generated by the mining activity have received the highest concern, as these plumes might travel for several kilometers distance from the mining activity. Various plume sources are identified, of which the most profound are those generated by the excavation and collection process of the seafloor mining tool and the discharge flow to be released from the surface operation vessel after initial dewatering of the ore. In this review, we explore the physical processes that govern plume dispersion phenomena (focusing in the main on benthic plumes), discuss the state of the art in plume dispersion analysis and highlight what lessons can be learned from shallow water applications, such as dredging, to better predict and reduce the spread and impact of deep-sea mining plumes.

Keywords: sediment transport, negatively-buoyant plumes, flocculation, aggregation, sediment spill

OPEN ACCESS

Edited by:
Daniel R. Parsons,
University of Hull, United Kingdom

Reviewed by:
Anabela Oliveira,
Instituto Hidrográfico, Portugal
Vera Van Lancker,
Royal Belgian Institute of Natural Sciences, Belgium

***Correspondence:**
Rudy Helmons
r.l.j.helmons@tudelft.nl

Specialty section:
This article was submitted to Marine Geoscience, a section of the journal Frontiers in Earth Science

Received: *03 February 2022*
Accepted: *25 April 2022*
Published: *19 May 2022*

Citation:
Helmons R, de Wit L, de Stigter H and Spearman J (2022) Dispersion of Benthic Plumes in Deep-Sea Mining: What Lessons Can Be Learned From Dredging? Front. Earth Sci. 10:868701. doi: 10.3389/feart.2022.868701

1 INTRODUCTION

The demand for critical raw materials, such as cobalt and rare earth elements is growing worldwide. This growth in demand is driven by the increasing world population and its increasing welfare, urbanization and development of technology (Hein et al., 2020). One of the main drivers nowadays is the electrification of the energy supply, e.g., cars, batteries, PV cells and wind-turbines. There is an increased global attention to the potential of deep-sea mineral deposits as an unexploited resource for various (critical) raw materials, and they is considered as a potential alternative to terrestrial deposits, hence they are of high economic interest (Wedding et al., 2015).

In general, three types of deposits, each with their own characteristics, are considered, i.e., polymetallic nodules, seafloor massive sulfides and cobalt-rich crusts. Polymetallic nodules are found on the surface of abyssal plains of the oceans, typically at water depths of 4–6 km. Polymetallic nodules are rich in metals and rare earth elements. The most extensive known nodule deposits are found in the Clarion Clipperton Fracture Zone (CCFZ) in the Pacific Ocean and the Indian Ocean Nodule Field (Hein et al., 2020). Seafloor massive sulphide (SMS) deposits are areas of hard substratum with high base metal and sulphide content that form through hydrothermal

circulation and are commonly found at hydrothermal vents. Such vents are typically found at tectonic plate boundaries and undersea volcanoes, e.g., Mid-Atlantic Ridge, Indian Ocean and Bismarck Sea (Boschen et al., 2013). Cobalt-rich crusts (CRC) are rock-like metalliferous mineral layers that form on the flanks of seamounts. Depending upon the concentration of metal compounds in the sea water, crusts with different thicknesses have formed in different ocean regions, ranging from 2 to 26 cm thickness. Most crusts have been found in the Prime Crust Zone (north-west Pacific), north-east of the Pacific Island states and Indian Ocean (Hein and Petersen, 2013).

While being of economic interest, these deposits are also essential habitats for benthic communities (Kaiser et al., 2017). Concerns exist on the recovery rate of the area affected by the mining activity (Gollner et al., 2017).

The structure of this paper is as follows. First, we provide an overview of a typical mining system and discuss the main comparisons and differences for the three main marine mineral deposit types. In the next chapter, we introduce the turbidity plume theory and apply it to plume sources originating from a seafloor mining tool, based on publicly available equipment properties. We will discuss relevant sediment properties and we will elaborate on to what extent particle aggregation might be of influence on the behavior of turbidity plumes. Next will be an analysis of how specific conditions at marine mineral deposits might be of influence on the generated turbidity plumes. Finally, we will take a closer look about what knowledge is currently lacking for deep-sea mining, but where we might benefit from experiences in shallow waters, e.g., in the field of dredging. This will be done mainly through analysis of near-bed turbidity discharges occurring from trailing suction hopper dredges. In addition, we will indicate what experiences from dredging might bring to the new field of deep-sea mining, aiming at improved prediction of plume dispersion and what might be done to minimize environmental impact caused by the equipment.

1.1 Mining Process

For each of the deposits, the lay-out of the entire mining system will be comparable. The ore is to be excavated and collected by one or more seafloor mining tools. For nodules, this pick-up process can be either hydraulic, mechanical or a combination of both. Typically, such collectors not only collect nodules, but also sediments and an excess of water. In the collector, nodules are to be separated from the entrained water. The excess of water and sediments will then be discharged as a plume behind the collector, which is often referred to as a collector plume.

In the case of SMS and CRC, the hard substrate needs to be excavated by rock cutting machines. So far, little is known about what particle size distribution is to be expected, especially to what extent fines (also referred to as fine sediment, here defined as having a grain size diameter <63 μm) will be generated, which will depend on rock properties, water depth and the excavation tool (Alvarez Grima et al., 2015; Helmons et al., 2016). As a result, little is known about the amount of fines that will be generated and spilled (not collected) by the seafloor mining tool. The spilled fines might result in a turbidity flow. To date there has been no deep-sea mining of SMS although the Solwara project, which concerned the mining of SMS in Papua New Guinea in 1,450–1,700 m water depth, progressed as far as a full Environmental Impact Assessment (Nautilus Minerals, 2008) and production of a full-scale mining plant. The project collapsed in 2019 when the developer, Nautilus, went into administration. There has been no full-scale mining of cobalt-rich crust to date although in July 2020 Japan Oil, Gas & Metals National Corporation (JOGMEC, 2020), successfully undertook test mining of cobalt-rich crust from the Takuyo No. 5 Seamount approximately 400 km east of Tokyo (JOGMEC, 2020).

The seafloor mining tool will feed the ore to a vertical transport system to transport the ore to surface. Once the stream of ore, water and remaining sediments arrives at the production support vessel, the ore needs to be dewatered and the excess water and sediment will be returned back to the deep sea, creating a discharge plume of fine particulate material (Oebius et al., 2001). Scenarios considered for the return water plume foresee that it will be released 1) in the water column below the thermocline, or 2) near the seabed (Washburn et al., 2019).

In the exploitation phase of nodule mining, a typical seafloor mining tool would have a width of 10–20 m and would move forward at a speed of approximately 0.3–0.5 m/s (Global Sea Mineral Resources NV, 2018). Estimations of seabed disturbance (or erosion depth) are in the region of 7 cm (Lang et al., 2019), but others state a range of potentially 5–15 cm (Global Sea Mineral Resources NV, 2018), or 10–15 cm (Nauru Ocean Resources Inc, 2021). Little information is publicly available regarding the estimated amount of excess water discharged by the collector system, these vary in the range of 125—375 L/s per meter width of a collector (Lang et al., 2019). Based on the estimated erosion depth and the discharge flow rate, a volumetric sediment concentration of approximately 1–3% is expected, which is equivalent to 25–80 g/L (initial bed porosities have been reported to be in the range of 0.8–0.9 (Jones, et al., 2021)). In the mining concepts published so far, independent of the choice of the collection method, the excess water and sediment will be discharged behind the mining vehicle, creating a plume of fine particulate material.

In the case of the near-bed generated plumes, i.e., nodule collector, SMS/CRC excavator or return water, sediment redeposition and bottom blanketing within the vicinity of the mining site could potentially bury benthic organisms, clog the respiratory surfaces of filter feeders and pollute the food supply for most benthic organisms. Both processes would affect the deep-sea ecosystem structure and functioning to a certain, although presently unknown, extent (Ramirez-Llodra, et al., 2011; Jones, et al., 2017). Currently, it is not yet known how large the affected area will turn out to be, and thus it is uncertain how severe the resulting environmental impact will be. From a technical point of view, it is of utmost importance to 1) be able to accurately predict where these plumes will travel and what deposition layer will be generated and 2) minimize the area affected by said near-bed plumes. Experience gained in turbidity management and analysis by the dredging industry can be of help to achieve aforementioned objectives.

2 TURBIDITY PLUME THEORY

The mixture of water, sediment and fine-grained nodule debris that is discharged behind the mining vehicle can be characterized as a negatively buoyant jet or plume. Due to its higher density, the plume will sink quickly to the seabed, from where it will propagate as a turbidity current. The following analysis is valid for any type of mining plume, but here special emphasis will be put on the sediment plume generated by a nodule collector (as this is the source of a turbidity plume that is best described in literature in terms of flow rate, concentration and the sediment properties). A similar approach can be used for other plume sources as well.

The source term exiting from the mining vehicle is characterized by its volume, momentum and buoyancy flux, in the frame of reference of the moving vehicle, defined as:

$$Q_{j0} = Au_{j0}$$
$$M_{j0} = \rho_{j0} Q_{j0} u_{j0}$$
$$g'_{j0} = g\frac{\rho_{j0} - \rho_{cf}}{\rho_{j0}}$$
$$B_{j0} = Q_{j0} g_{j0}'$$

With the volume flux exiting from the discharge Q_{j0}, cross-sectional area A, initial discharge velocity u_{j0}, initial momentum flux M_{j0}, discharge density ρ_{j0}, ambient density ρ_{cf}, reduced gravity g'_{j0}, gravity g, and initial buoyancy flux B_{j0}. It is worth mentioning, that in the case of an operational mining vehicle, the source is moving, discharging at an approximate neutral velocity. This is envisaged by adjusting the discharge opening to accommodate a similar discharge velocity of the mixture opposing the forward velocity of the mining tool, aiming for a minimum net momentum. The conditions of the flow exiting from the vehicle diffusers can be described with Reynolds Re, densimetric Froude Fr , Richardson Ri numbers, and the ratio of net vehicle-discharge velocity relative to the current velocity ratio (square root of the momentum ratio) γ, respectively given by

$$Re = \frac{\rho_{j0} u_{j0} H}{\mu}$$
$$Fr = \frac{u_{j0}}{\sqrt{g_0' H}}$$
$$Ri = \frac{g_0' H}{u_{j0}^2}$$
$$\gamma = \sqrt{\frac{\rho_{j0}\left(u_{j0} - u_v\right)^2}{\rho_{cf} u_{cf}^2}}$$

With height of the discharge opening H, vehicle velocity u_v and dynamic viscosity μ.

For Re > 10^4, the outflowing mixture will be turbulent. As long as the jet starts fully turbulent, mixing of the jet is not strongly affected by the jet Reynolds number (Jirka, 2007) but it is primarily governed by Ri (equal to $1/Fr^2$) and γ. For Fr < 1 the outflow is subcritical, for Fr > 1 the outflow is supercritical.

TABLE 1 | Range of dimensionless numbers for the discharge conditions. Values are based on design specifications,–indicates lower bound, + indicates upper bound for concentration c (0.01–0.03) (mol/L), vehicle velocity v (0.25–0.5) [m/s] and discharged volume Q (0.125–0.375) [m^3/s per meter width]. Values are taken from (Lang et al., 2019).

	Re	Fr	Ri	$\frac{l_s}{H}$	$\frac{l_m}{H}$
c–, v–, Q-	13255	0.96	1.08	11885	1.14
c–, v+, Q-	6627	1.36	0.54	37733	3.85
c–, v–, Q+	39765	0.56	3.24	8241	0.50
c– v+, Q+	19883	0.79	1.62	26162	1.69
c+, v–, Q–	27230	1.11	0.81	12099	0.66
c+, v+, Q-	13615	1.57	0.41	38413	2.22
c+, v–, Q+	81690	0.64	2.40	8389	0.29
c+, v+, Q+	40845	0.91	1.22	26634	0.97

For Ri < 1, the flow is dominated by momentum, for Ri > 1 the flow is dominated by buoyancy. Based on the numbers provided by (Lang et al., 2019), the range of the dimensionless numbers is provided in **Table 1**. The current velocities close to the seabed in the abyssal plains are generally rather low, with typical mean current velocities in the range of 5–15 cm/s (Gillard et al., 2019). During the mining operation, it must be assumed that the current can come from any direction, cross or parallel.

It remains to be seen how the mining systems will perform operationally. However, based on the analysis of the Froude and Richardson number, some regime changes, e.g., sub- or supercritical flow being discharged from the mining collector. In the case where the outflow is subcritical (Fr < 1), the mixture will automatically redistribute to arrive at $Fr = 1$ with a discharge at higher concentration and velocity in the lower half of its height compared to the upper part of the discharge. In severe cases, water from the environment can even flow into the discharge. As a result, the assumed neutral exit velocity does not hold and thus the outflow maintains more energy than anticipated. To minimize the chance of heterogeneous outflow, various options are available, e.g., guided vanes and/or vortex generators.

2.1 Length Scales

Initially the horizontal momentum is important, but eventually (negative) buoyancy will force the flow towards the seabed. After impinging on the bed, it will continue as a turbidity current. Various regimes can be distinguished for a (negatively) buoyant jet in crossflow (Fischer et al., 1979). An x-z reference frame is used, i.e., x is in horizontal direction and z is in vertical direction.Within a distance of $z < l_m$ from the source a buoyant jet acts as a jet and when $z > l_m$ a buoyant jet acts as a plume. A length scale z_M is defined for the influence of the initial momentum compared to the ambient current. Length scale z_B is defined for the influence of the initial buoyancy, when $z < z_B$ initial buoyancy is dominant over the ambient current. These length scales are given by

$$l_m = \frac{\left(Q_{j0} u_{j0}\right)^{3/4}}{\sqrt{B_{j0}}}$$
$$z_M = \frac{\sqrt{Q_{j0} u_{j0}}}{u_{cf}}$$

$$z_B = \frac{B_{j0}}{u_{cf}^3}$$

See **Figure 1** for a sketch of the different flow regimes in relation to the different length scales. As the discharged flow is sediment laden, an additional length scale can be defined, based on the jet momentum flux and the particle settling velocity

$$l_s = \frac{M_{j0}^{2/3}}{w_s}$$

This length scale plays an important role in the analysis of the sedimentation spatial variation. The horizontal distance when particle fallout first occurs can be linearly correlated to l_s. A larger value suggests that the particles mainly follow the plume trajectory, while low values of l_s result in settling velocity dominating the flow response.

According to experiments performed by (Lee et al., 2013), the particle concentration contours may be divided into three regions. For $x < 0.5l_s$, the sediment jets behave like a pure jet with concentric contours. For $0.5l_s < x < l_s$, the sediment cloud starts to depart from the water jet and for $x > l_s$, the particle jet is separated significantly from the water jet. They also found a longitudinal deposition rate F_s based on l_s. According to their experiments, sediment starts to fall out of the jet at approximately $x/l_s \approx 0.2 - 0.3$, the peak deposition rate at approximately $x = 0.93\, l_s$ and at $x = 2.4l_s$ over 90% of the sediment input has settled. It has to be noted, that these experiments have been conducted for various narrow particle size distributions consisting of sand or glass spheres.

Laboratory experiments for horizontal sediment-laden plumes have been conducted by (Bleninger, 2000) and (Neves et al., 2002) who conducted experiments where the sediment deposition was found to be log-normal distributed. These experiments were coupled with dimensional analysis to determine the deposition rate of small particles based on a momentum-settling length scale.

(Cuthbertson et al., 2008) and (Liu and Lam, 2013) demonstrated experimentally and numerically that for initial sediment concentrations below 0.1% of volume, no significant changes to the properties of the jet flow are noticeable. For jets with higher initial sediment concentrations, the settling of particles is observed to drag the jet with a downward bending trajectory.

It is worth noting that hardly any publications so far have taken into consideration that in the case of a mining vehicle for the collection of polymetallic nodules, the vehicle will be moving. The research conducted in laboratory seems to be entirely based on stationary jets.

The work of (Decrop and De Wachter, 2019) is only one of the very few public articles that address the effect of the moving vehicle on the discharged sediment plume. This work is based on a Computational Fluid Dynamics (CFD) model based on Reynolds Averaged Navier Stokes (RANS) turbulence modelling. In this work, various vehicle scenarios are considered, mainly for different vehicle velocities and discharge conditions. It also considers the effect of the wake of the vehicle in the initial mixing phase. So far, no validation through experiments has been provided.

Recently, (Ouillon et al., 2021) presented research on gravity currents originating from moving sources. In their research, they conducted experiments in a towing tank where a model collector discharges a dense dyed fluid in its wake. These experiments have been used to validate CFD results based on Direct Numerical Simulations (DNS). It is identified that the ratio of the speed of the source (mining vehicle) to buoyancy velocity can be used to define sub- and supercritical gravity current formation. In the case of supercritical flow (where the mining vehicle is able to stay in front of its own generated turbidity current), a wedge-shaped gravity current occurs behind the collector. In this supercritical regime, the turbidity current goes through a second transition in which the head of the turbidity current moves approximately normal to the vehicle's direction, and the time evolution of the front in lateral direction tends to be comparable to a constant volume lock-release gravity current. Their research provides valuable insights on the near-field behavior of the mining vehicle plumes. For obvious reasons, their experiments have not considered the presence of actual sediments in the discharged flow. The effects of sediments will be discussed in the next section.

2.2 Deep-Sea Sediments

Where coastal and shelf sediments usually are predominantly composed of lithogenic clay, silt and sand produced by weathering and erosion of the adjacent land mass (except on subtropical and tropical carbonate shelves), deep-sea sediments encountered at sites of potential DSM are usually a mixture of clay and silt transported from distant land masses by ocean currents or wind, or produced by weathering of oceanic rock, and silt to sand-sized skeletal remains of mostly pelagic organisms composed of carbonate (mostly coccolithophores and planktonic foraminifera) or silica (mostly diatoms and radiolarians). Volcanic debris and authigenic minerals precipitated from seawater or local pore water contribute a relatively minor fraction, with areas rich in polymetallic sulphide or oxide precipitates as a notable exception. On the crests of mid-ocean ridges and seamounts, enhanced bottom currents associated with internal waves often winnow out the finest sediment fractions, producing a relatively coarse-grained

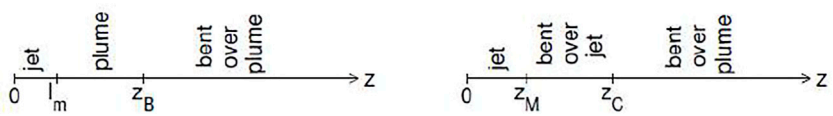

FIGURE 1 | Length scales and flow regimes of a buoyant jet in cross flow in case $z_B > z_M$ (**left**) **or in case** $z_M > z_B$ (**right**) with $z_C = z_M (\frac{z_M}{z_B})^{1/3}$, (de Wit, 2015).

TABLE 2 | Fraction distribution of sediments. GSR and NTNU data from (Lang et al., 2019), IOM data from (Zawadzki et al., 2020). Averaged data is provided by Global Sea Resources, based on the Belgium license area in the CCFZ, NTNU data is data of specific box-cores of the GSR data average. IOM data is based on data of the Inter Ocean Metal license area in the CCFZ.

Fraction	Diameter range (μm)	GSR data average (%)	NTNU data BC062 (%)	NTNU data BC064 (%)	IOM data average (%)	Gillard et al. (2019)
Clay	< 2	12.0	11.3	14.5	23.24	25.3
Silt	2—63	76.2	85.7	82.5	70.36	52.11
Sand	63—2000	11.8	3	3	6.13	22.5

TABLE 3 | Percentages of mineral groups in deep-sea sediment. IOM data from (Zawadzki et al., 2020), GSR data from (Global Sea Mineral Resources NV, 2018), Sites A-C (Bisschof et al., 1979). Note that for IOM 1, 2, 3, clay mineral % is given relative to total sediment. For Site A, B, C and GSR clay mineral % is relative to sum of clay minerals only.

	IOM 1	IOM 2	IOM 3	Site A	Site B	Site C	GSR	IOM
Smectite (%)	12.71	17.33	16.49	52	38	40	36.41	16.3
Illite (%)	13.82	12.05	14.25	31	42	50	48.34	13.2
Kaolinite (%)	0.65	0.43	0.54	17	20	10	10.33	1
Chlorite (%)	1.7	1.85	2.35				4.92	1.5
Amorphic (%)	50.47	47.09	44.42					

residue. Corals, sponges and other benthic megafauna which at these sites find favourable conditions for nutrition, often produce a significant amount of coarse-grained bioclastic sediment. In contrast, sediment of the abyssal plains is mostly very fine grained, reflecting the sluggish bottom current regime. Characteristic particle size distributions in nodule-rich areas are presented by (Lang et al., 2019; Zawadzki et al., 2020), see **Table 2**. The local clay composition varies to a larger extent. However, in all publicly reported cases, smectite and illite are the most abundant, see **Table 3**.

Since large parts of the abyssal seafloor are located well below the carbonate compensation depth (CCD), biogenic carbonate settling out from the euphotic zone is mostly not preserved. The deep-sea clay is therefore typically poor in carbonate, and predominantly composed of a mixture of clay minerals and siliceous remains of plankton like diatoms and radiolarians. Only below biologically productive surface waters such as the equatorial upwelling zones, where the supply of biogenic carbonate exceeds the dissolution below the CCD, is carbonate preserved in the sediment.

The supply of fresh organic matter to the seabed, which may play an important role in the aggregation of suspended sediment (Fettweis and Baeye, 2015), varies greatly depending on the overall productivity regime of the surface water and the water depth. In general, organic matter flux to the seabed decreases with increasing water depth due to progressive degradation and remineralisation of organic matter as it sinks to greater depths. Seamounts reaching to shallow depths below biologically productive surface waters receive an orders of magnitude higher flux of fresh organic matter than abyssal plains. As is clearly reflected by abundance and biomass of benthic life depending on the vertical flux of organic matter. The upper few centimeters of the sediment in the CCFZ have a carbon content of less than 0.5% of the mass of the sediment. Below 30 cm, this declines to 0.1% of the mass of the sediment (Volz et al., 2018).

2.3 Sediment Flocculation and Cohesive Sediment

The discharge flow of the nodule collection vehicle is expected to consist of sediment, water and nodule debris. It might be assumed that the nodule debris exiting from the discharge has a significantly larger settling velocity than that of the sediment, and that this nodule debris will settle close by. The exact composition of the discharged flow will strongly depend on the nodule collection method and separation method that is used to separate the nodules from the excess of water entering the collector. Under influence of turbulence, differences in settling velocity and Brownian motion, mud particles can cluster together to form flocs with typical sizes of 0.05—1 mm (Gillard et al., 2019). The density of the flocs is less than the density of the individual particles, but the settling velocity is larger. Flocculation is especially relevant when the mud concentration is large. In shallow water, Strong flocculation effects have been found for mud fractions in the overflow dredge plume of a TSHD, with floc diameters of 40–800 micron and floc settling velocities of 0.1–6 mm/s (Smith and Friedrichs, 2011). Similar floc settling velocities have been found for CCFZ sediment by (Gillard et al., 2019).

As shown in **Table 3**, the clay fraction of CCFZ sediment mainly consists of smectite (montmorillonite) and illite. Smectite particles are relatively small and have a large specific surface area (SSA, which is defined as the ratio of the surface area of a material to either its volume or mass (Baker et al., 2017). The SSA affects the magnitude of the interparticle forces, where larger SSA leads to larger interparticle forces (Atkinson, 2017). The SSA of smectite is further enhanced by its ability to absorb water into

TABLE 4 | Typical values of thickness, planar diameter, specific surface area and cation exchange capacity for common clay minerals (Yong et al., 2012).

Edge view	Typical thickness (nm)	Planar diameter (nm)	Specific surface area (m^2/kg)	Cation exchange capacity (mEq/100 g)
Montmorillonite	2	10–1,000	700–800	80–100
Illite	20	100–2000	80–120	10–40
Chlorite	30	100–2000	70–90	10–40
Kaolinite	100	10–1,000	10–15	3–15

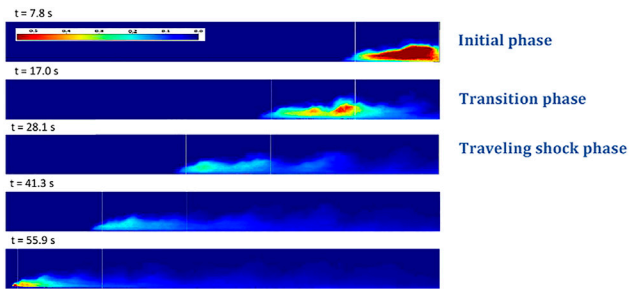

FIGURE 2 | Results of low concentration suspended sediment lock-exchange experiment, depicting the different phases of a particle-driven current, (Helmons et al., 2019)

its crystal lattice structure (Yong et al., 2012), see **Table 4**. The cation exchange capacity (CEC) provides the potential chemical activity of a clay mineral, which in turn is directly related to the magnitude of the cohesive forces. For higher CEC, the clay will behave more plastic and higher cohesive and adhesive shear strengths may be expected as well (Kooistra et al., 1998; Baker et al., 2017).

2.4 Particle-Driven Gravity Currents

After the impinging on the seabed, the remaining plume will continue as a particle-driven gravity current. While the current spreads, particles fall out and the effective driving strength of the current, compared to a homogeneous current, decays (Ungarish, 2009). Alternatively, sediment may be entrained if the current is passing sufficiently rapid over an erodible bed, which will increase the particle concentration and thus the driving buoyancy force.

The behavior of the resulting particle-driven current can be divided into three phases, i.e., the initial or starting phase, the transition phase and a traveling shock phase, see **Figure 2**. During the initial or starting phase, the initial volume of the current collapses, which typically happens in the impingement region. In the transition phase, the height of the nose increases and the particle concentration is declining faster in the tail than at the head. In the last phase, the traveling shock phase, a bore is

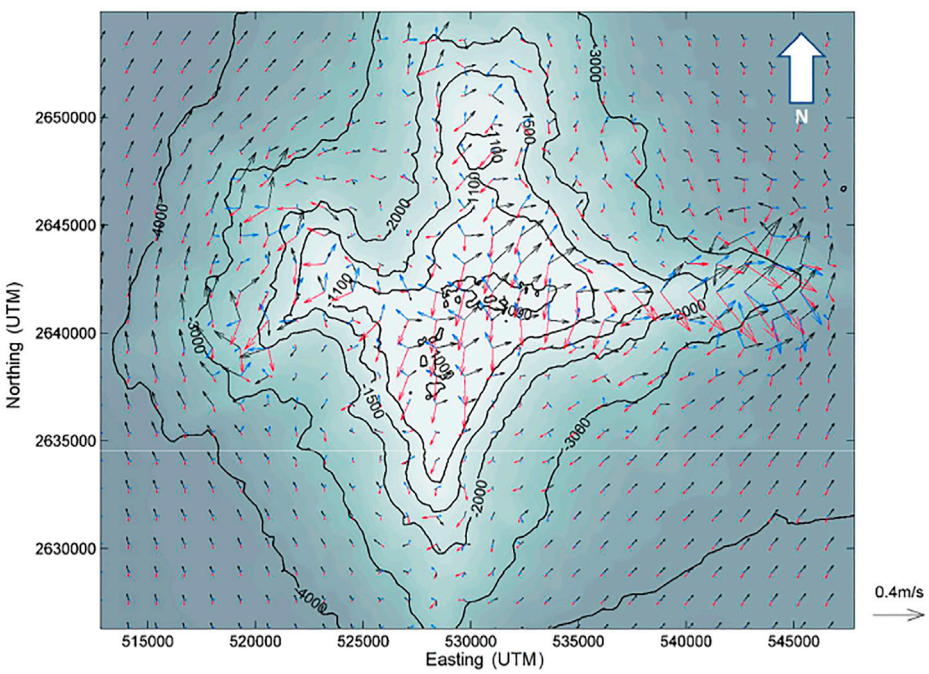

FIGURE 3 | Snapshots of currents 10 m above the bed in the vicinity of the Tropic Seamount, during a spring tide at HW (black), HW+4 h (ref) and HW+8 h (blue) (Spearman et al., 2020).

developed within the current, which rapidly changes the height and velocity of the current (Bonneaze et al., 1993).

(Gladstone et al., 1998) conducted non-cohesive lock exchange experiments (where fluids of higher density, in this case due to suspensions of particles, are released into fluids of lower density) with bi-disperse particle size distributions. They found that the mixing of different sizes of particles has a strong non-linear effect on both the motion of the current and the sedimentation patterns. Adding small amounts of coarse particles to a current composed of small particles has little effect on the dynamics of the current. In the opposite case, adding a fraction of fine particles to a dominantly coarse material has a significant effect as the flow will travel further and will be able to maintain its velocity for a longer duration. This non-linearity arises from the presence of modest amounts of fines which cause the current to maintain an excess density difference for a longer time. The decay of velocity is dominated by particle settling, which is reduced by the presence of fines. In conclusion, the transport of bi-disperse and poly-disperse mixtures depends strongly on the amount of fines present.

(Marr et al., 2001) conducted experiments of cohesive sand-rich sub-aqueous gravity flows in a flume which also carried bentonite or kaolinite. They found that between 0.7 and 5% by mass bentonite was sufficient to produce coherent flows, compared with 7% for kaolinite.

In their definition, coherent flows are flows that resist breaking apart and becoming completely turbulent under the dynamic stress associated with the head of the propagating gravity flow. That this phenomenon occurs for lower concentrations of bentonite is caused by the mixtures' higher yield strength. (Baas et al., 2016) found similar results in channel flow experiments of low concentration kaolinite and bentonite mixtures.

(Baker et al., 2017) conducted lock exchange experiments for various concentrations and clay types, i.e., silica flour, kaolinite and bentonite, all in ambient seawater. Based on these experimental results, there is no significant difference in flow response for low concentrations of sediment. For volumetric concentrations of 10% for bentonite, 15% for kaolinite and up to 44% for silica flour, the resulting flow exhibits strong turbulent mixing. The only significant differences for comparable initial densities would be the result of the effective settling velocity of the sediment used. In the case of volumetric concentrations >15% for kaolinite and >10% for bentonite, the flow behavior is affected by gelling of the mixture.

3 DEEP-SEA MINING

3.1 Deep-Sea Conditions

In dredging operations in coastal waters, the dispersion of the sediment plume in vertical direction is often confined within a few metres to tens of metres between the sea surface and the seabed. In deeper waters of the shelf, strong vertical density gradients associated with a seasonal or permanent thermocline and present below the upper few tens of metres of mixed surface water, may also limit the vertical dispersion of plumes. Spreading of the plume in coastal and shelf waters thus occurs mostly in horizontal direction by relatively strong wind- or tide-driven currents, whilst turbulence makes the plume expand vertically within the boundaries set by sea surface, seabed and density stratification. Plumes generated by DSM, in contrast, are much less vertically confined.

Although density stratification is normally also present in waters below the thermocline, it is less strongly present than in shallower waters. Especially in their initial phase after release, sediment plumes have substantial excess density relative to the water of the receiving environment, which will make the plume sink vertically if released in open water or roll downslope as a turbidity current if released above a sloping seabed. Thus, DSM plumes may spread out over a considerable vertical distance before mixing with ambient water slows down their descent. In addition to the negative buoyancy of the plume itself, vertical dispersion may be further enhanced by vertical water motions induced by internal waves. These are oscillations within a water mass produced when stratified water flows over abrupt seabed topography, such as typically the case at the shelf break, or on mid-ocean ridges or isolated seamounts. Internal waves may induce large vertical water mass motions of more than 100 m in the ocean interior, and especially where they break they produce strong turbulence and water mass mixing (van Haren and Gostiaux, 2012; van Haren et al., 2017) although they may also lead to hydrodynamic conditions which hinder the wider dispersion of sediment plumes, such as tidally rotating currents (Spearman et al., 2020). Internal waves are thus an important factor to be taken into account when considering plume dispersion for DSM in topographically complex terrain, such as mining of SMS and polymetallic crusts (both deposit types are typically found at or near seamounts). But even in abyssal plain settings, away from major topographic features, significant turbulence and mixing has been observed, generated by internal waves produced over abyssal hills (van Haren, 2018).

3.2 Return Flow of Sediments, Waste and Other Effluents

In all types of DSM, ore slurry pumped up from the seabed through the riser system needs to be dewatered to allow safe storage on board of the mining vessel. Subsequent transfer of the ore to a bulk carrier for transport to land will require a second dewatering step, if the ship-to-ship ore transfer is done in a slurrified state. The dewatering on board of the mining vessel may also involve further separation of valuable ore from unwanted sediment entrained in the flow. The excess water produced in the dewatering process, loaded with sediment and also the fine-grained ore fraction that cannot be retrieved by sieving and centrifugation, will have to be returned back to sea, creating a discharge plume of fine particulate material (Oebius et al., 2001). In the case of nodule mining, the amount of fine-grained material discharged from the mining vessel may be substantial. The total discharge of water and solids has been estimated previously at 50,000 m^3 per day, with a solids concentration on the order of 10 kg/m^3 (Oebius et al., 2001). More recent estimates give an order of magnitude higher numbers for total discharge and solids

concentration (Lang et al., 2019). According to the latter, fine-grained sediment entrained with the nodules will make up the bulk of the solid material discharged. Nodule fines, produced by abrasion and fragmentation of nodules during pickup, vertical transport and dewatering, and too small to be retrieved during on-board processing, would constitute only a few percent of the solid mass. In the case of SMS and crust mining, any sediment overburden will likely be removed prior to ore excavation, and the excavated material pumped up as a slurry to the mining vessel will thus consist predominantly of valuable ore. The solids discharged with dewatering fluid will likewise consist mostly of fine-grained ore material. Estimates of total dewatering discharge for SMS mining are between 22,000 and 38,000 m^3 per day (Nautilus Minerals, 2008; Okamoto et al., 2019). The only available estimate of solids concentration is from the Nautilus Solwara EIA which was estimated as around 6 kg/m^3 (Nautilus Minerals, 2008).

Discharge of dewatering water and solids directly at the surface is expected to have multiple and potentially harmful impacts on surface ocean pelagic life, such as shading out of photosynthesizing plankton, phytoplankton blooms due to input of mineral nutrients, clogging of feeding apparatus of pelagic suspension feeders, reduced buoyancy of plankton, reduced visibility interfering with predators hunting on sight, toxic effects of trace metals released from ore particles. To avoid these impacts, ISA draft regulations for exploitation of polymetallic nodules (Lenoble, 2000) prescribe that water and solids should be discharged below 1,000 m water depth, well below the biologically productive sunlit surface ocean layer, and below the steep density gradient of the permanent thermocline which will impede return of the discharged material to the surface. (Munoz-Royo et al., 2021) have studied such a mid-water plume in dynamic discharge experiments at approx. 60 m water depth with mixtures based on CCFZ sediment. They identified that its vertical and horizontal extent is notably influenced by 1) the amount of discharged sediment and 2) background turbulent diffusivity. Another key finding in their work is that flocculation of sediment does not play a notable role due to initially high turbulent shear rates near the discharge opening and low concentration downstream due to rapid turbulent entrainment.

However, (Drazen, et al., 2020) have pointed out that there is a wide variety of pelagic life also below 1,000 m depth, which will be impacted likewise by discharge plumes. The authors argue that the pelagic ecosystems should be an integral part of environmental impact assessment and environmental monitoring plans. To mitigate impacts on pelagic life, they suggest delivering the discharge to the seafloor where a sediment plume will already exist from seafloor activities. This would result in additional pressure on benthic organisms but would relieve pressures on the mid-water ecosystem.

Releasing the dewatering discharge at short distance above the seabed brings about the risk that erosive turbidity currents are generated at the point where the plume impinges on the seabed, due to initial momentum of the discharge and the relatively high excess density relative to the ambient deep-sea water (van Grunsven et al., 2018). In the path of the turbidity current, the seabed may be stripped of the surface sediment layer including benthic life and organic material serving as primary food resource for the benthos, whereas the resuspended sediment will be dispersed and settle out downslope, aggravating the impact of the plume generated by the mining vehicle. Adjustment of the discharge height above the seabed and the direction of the discharge jet and a diffuser may help to prevent or reduce the formation of erosive turbidity currents.

3.3 Plume Generation When Mining Seafloor Massive Sulphides and Cobalt-Rich Crusts

Sea-floor massive sulphides (SMS) are deposits of metal-bearing minerals that form on and below the seabed as a consequence of the interaction of seawater with magma below the seabed. During this process, cold seawater penetrates through cracks in the sea floor and is heated to high temperatures causing metals to be leached out from the surrounding rock. The resulting chemical reactions that take place in this process result in seawater enriched in dissolved metals and sulphur. Due to the lower density of this evolved seawater, it rises rapidly to the sea floor, where most of it is expelled into the overlying water column as focused flow at chimney vent sites. The dissolved metals precipitate when the fluid mixes with cold seawater. Much of the metal is transported in the hydrothermal plume and is deposited as fallout of particulate debris. The remainder of the metal precipitates as metal sulphides and sulphates, producing black and white smoker chimneys (Baker and Beaudoin, 2013).

Fe–Mn crusts occur on hard-rock substrates throughout the ocean basins. They form at the seabed on the flanks and summits of seamounts, ridges, and plateaus where the rocks are largely depleted of sediment (Hein and Koschinsky, 2014). The most metal-rich crusts occur at depths of about 800–2500 m (Hein and Petersen, 2013). The thickest crusts on individual seamounts commonly occur on outer-rim summit terraces and broad saddles on the summit of guyots (flat-topped seamounts).

3.3.1 Estimating the Loss of Crust/SMS Particles Into the Water Column

Crust and SMS plumes are in principle similar to those arising from dredging of weak rock (crusts; (Yamazaki et al., 1995) and moderately strong rock (SMS; (Spagnoli et al., 2014) by cutter suction dredger (CSD) in shallow waters (Spearman et al., 2020). The near-field processes which contribute to losses from CSD are complex and difficult to model numerically. However, a reasonable estimate of the resulting loss of fines can be established by using standard dredging industry approaches, e.g., (den Burger, 2003; Becker, et al., 2015), based on field and laboratory measurements, to estimating cutter suction losses. (van Wijk et al., 2019) showed that polymetallic nodules can fragment upon impact with (in) the mining equipment, potentially complicating preliminary subsea separation processes. It should be pointed out that for mining, particles lost to the surroundings represent a loss of resource and there is an incentive for the developer to reduce these losses further, as much as is practically possible, through design of the mining plant.

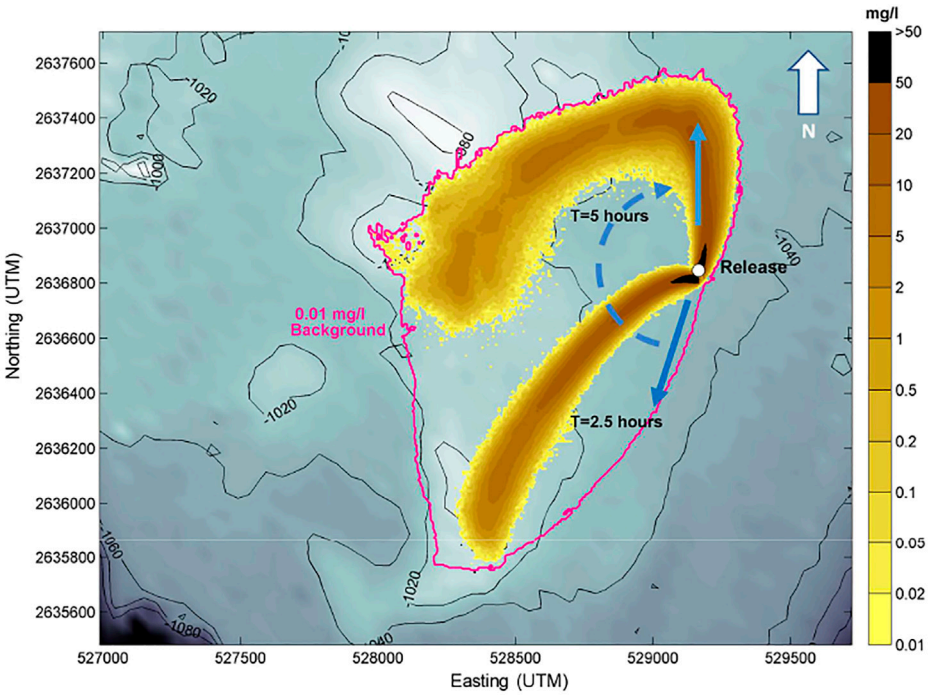

FIGURE 4 | Snapshots of predicted increases in suspended sediment concentration (averaged over bottom 10 m of water column) resulting from 5-h simulation of mining on the Tropic Seamount with representative rates of release. Snapshots shown at +2.5 h and +5 h. Envelope of increases greater than 0.01 mg/L (equivalent to background) over whole of simulation are indicated by magenta line (Spearman et al., 2020).

3.3.2 Effect of Topography on Hydrodynamics

Cobalt-rich crusts occur on the summits and sides of seamounts (and other similar topographical features) which exhibit specific dominating hydrodynamic features, including Taylor caps, an isolated region of flow situated above the seamount, and internal tides, where surface tides move stratified water up and down sloping topography, producing a wave in the ocean interior (Lavelle and Mohn, 2010). SMS fields also commonly occur on ridge features with steep slopes and display great variation in bathymetry, which can result in similar hydrodynamic features. The nature of the resulting hydrodynamics will always be site-specific but the typical features are here discussed using the results of the Marine E-tech project (Spearman et al., 2020) which investigated the hydrodynamics (as well as the topography, geology, geochemistry, ecology and potential mining plume dispersion) in the vicinity of the Tropic Seamount around 300 nautical miles SSW of the Canary Islands. The seamount has a star-shaped platform with a width of approximately 40 km at the base and about 15 km at the crest. Its summit rises 3,000 m from the abyssal floor to a depth of ~1,000 m where it forms a flat plateau partially covered by mobile sediment deposits of silty sand, with the remainder being covered by pavement crusts see **Figure 3**.

The currents just above the surface of the Tropic Seamount were observed to be dominated by internal tide-generated currents that rotate in an anti-cyclonic direction about the seamount's centre. Validated hydrodynamic modelling (using the TELEMAC modelling suite, *opentelemac.org*) identified that current speeds (driven by internal tides) varied up to 0.3 m/s, with the highest values on the east and west "spurs" of the seamount, and that a weak Taylor cap exists around the seamount, close to the seabed. The tidal variation was observed to be semi-diurnal but transfer of energy via sub-harmonic resonance from the semi-diurnal internal tidal harmonic can also result (as here) in significant diurnal components of current flow, even though there is minimal external diurnal influence (Gerkema et al., 2006; van Haren et al., 2010).

The rotating currents found at the seamount were identified in the Marine E-tech project as one of the key processes limiting the dispersion of fine sediment from a (potential) mining source. **Figure 4** shows the results of a 5-h simulation of continual release of fine sediment, (Spearman et al., 2020). The figure shows snapshots of the plume (here at 2½ and 5 h) and the envelope of predicted increases in suspended sediment concentration above 0.01 mg/L (which represents the background sediment concentration). During the simulation, the current starts in a SSW direction and rotates clockwise, finishing in a north direction by the end of the simulation. The figure shows that the excursion of the plume towards the west and south (the principal direction of the currents during the simulation) is limited to around 1.4 km due to the combination of rotating tidal currents. This result indicates the importance of reproducing tidal processes in deep-sea mining studies, at least where they interact with bathymetry

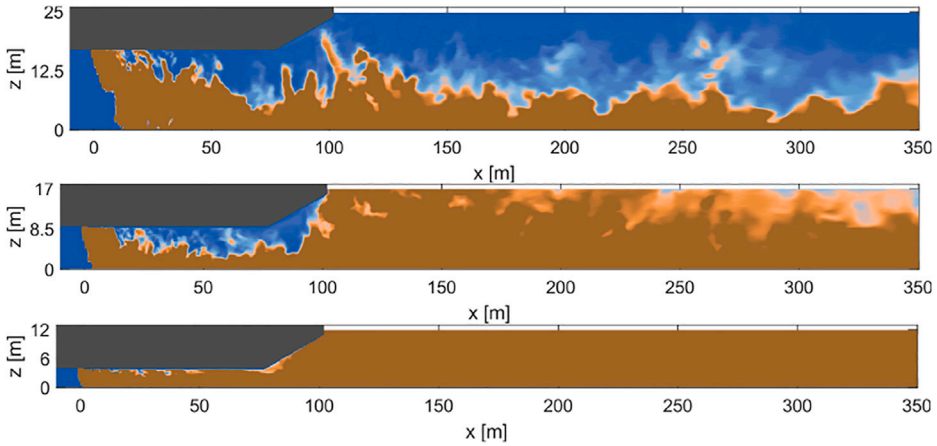

FIGURE 5 | Illustration of the influence of the depth/under keel clearance on TSHD overflow dredge plume mixing (de Wit et al., 2014a, b) for three different depths with all else similar (Ri = 1.2 and γ = 1.3). The propellers of the TSHD are included in the simulation and by entrainment pull some of the plume upward.

and density gradients to induce currents much larger than those normally associated with the deep ocean.

3.3.3 Effect of Substrate Type

While little research has been undertaken on the flocculation of debris particles likely to result from SMS mining, detailed video-imaging tests (LabSFloc-2 high resolution video-technology, (Manning and Dyer, 2007) of cobalt-rich crust debris in *in situ* seawater strongly indicates that crust particles flocculate more readily than normal sediment particles (including the clay/silt ooze found in the CCFZ—see Section 1.2). The Marine E-tech project (Spearman et al., 2020) found that, due to flocculation processes, 57% of particles less than 63 microns settled at a rate of around 10 mm/s with only 3.5% of particles settling at less than 0.1 mm/s. Like the rotational effect of internal tides, this strong flocculation effect causes a significant reduction in the dispersion of the benthic plume caused by mining.

4 SHALLOW WATER APPLICATIONS (DREDGING)

So far, we have discussed the most relevant aspects of deep-sea mining turbidity flows. In this section we will discuss how turbidity flows occur in shallow water applications like dredging (and wet mining). While dredging sediment plumes can be generated and dispersed to surrounding areas, just like when executing DSM. The dredging industry is well established and dredging projects take place all over the world. The environmental impact of dredging, often with dredge plumes as important component, has been the source of research for many decades, e.g. (Pagliai et al., 1985; Nichols et al., 1990; Bray, 2008; Erftemeijer et al., 2012; Laboyrie and Kolman, 2018). Knowledge gained from dredge plumes is used in this section to learn lessons for DSM plume modelling. Specific focus is made here on Trailing Suction Hopper Dredger (TSHD) overflow plumes as a TSHD is an often-used type of dredge equipment and TSHD overflow plumes bear similarities with DSM plumes because both are generated by moving equipment.

4.1 Overflow Plume (Near Field)

A TSHD is a high production dredging plant, which is often used for both maintenance dredging (e.g., recurrent dredging to maintain or improve existing waterways) and capital dredging (e.g., dredging in a new location and in material that has not been dredged before, such as land reclamation, deepening and widening channels). The overflow plume is generally the most important source of turbidity while dredging with a TSHD (Bray, 2008; Laboyrie and Kolman, 2018). A TSHD overflow dredge plume is generated while loading a TSHD and letting the excess process water overboard. Typically, overflow is done via a vertical pipe in the hopper which ends at the keel of the vessel, see **Figure 5** for an impression. During loading and overflowing a TSHD is moving. For TSHD overflow dredge plumes both initial buoyancy and initial momentum are important. The sediment release is downward, perpendicular to the crossflow which is formed by the combination of sailing speed and ambient current velocity. The outflow velocity is often in the same order of magnitude as the crossflow velocity. This is illustrated by the typical velocity ratios and Richardson numbers of $\gamma = 0.3 - 4$ and $Ri = 0.01 - 22$ (de Wit et al., 2014a, b; Decrop, 2015). Near-field TSHD overflow plumes can behave dynamically driven by negative buoyancy, while more diluted ones behave passively driven by ambient currents (Winterwerp, 2002). Far away from the dredger all overflow plumes are diluted so much that they end up as passively driven. Especially at the end of loading a TSHD the overflow discharge density can be high, growing to more than 400 kg/m^3 sediment concentration (van Rhee, 2002; Spearman et al., 2011; Spearman, 2014).

When dredging in deeper waters the distance from the release point at the keel of a TSHD and seabed is large, and the plume will descend under influence of its excess density and initial downward momentum. But when dredging in shallower water the seabed is rather close and the propellers driving a TSHD can

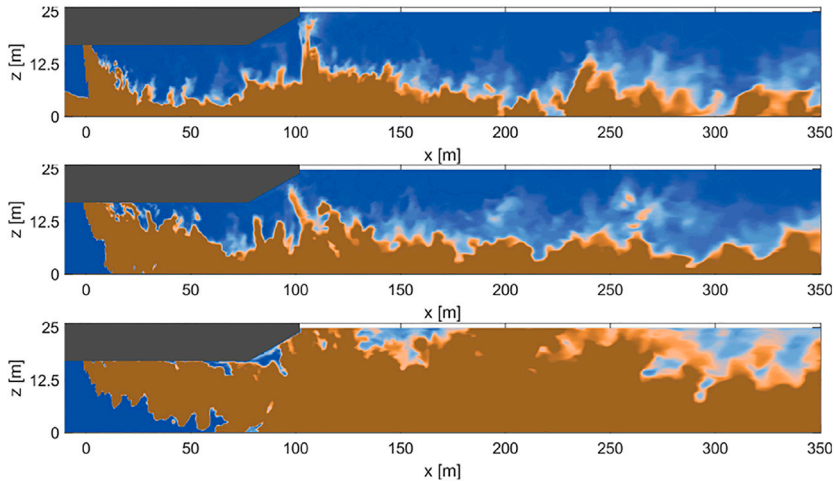

FIGURE 6 | Illustration of the influence of the crossflow velocity on TSHD overflow dredge plume mixing (de Wit et al., 2014a, b) for three different u_{cf} (0.5 m/s, 1.5 m/s and 3 m/s respectively, $\gamma = 0.6$ $\gamma = 1.3$ $\gamma = 3.8$) with all else similar (Ri = 1.2). The propellers of the TSHD are included in the simulation and by entrainment pull some of the plume upward.

impact the plume behavior seriously by entraining the sediment plume upwards to the water surface (de Wit et al., 2014a, b). In addition, when a TSHD is sailing fast with respect to the ambient current direction the upward movement of the plume to the water surface is helped by the upward flow at the aft of the TSHD hull. An example of the influence of the distance from release point and seabed on TSHD overflow plume mixing is shown in **Figure 5** and an example of the influence of the crossflow magnitude is given in **Figure 6**.

This clearly illustrates how the equipment generating a plume and interaction between plume and immediate surroundings can significantly impact the resulting plume behavior. Also, for DSM this should be considered when assessing plume dispersion. Although mixing up a sediment plume all the way to the water surface, like for TSHD plumes, is not possible for DSM plumes, also for DSM plumes some additional mixing up by either the equipment movement, its wake, or by the local details how the plume is released can impact the travel distance and concentrations significantly. Details of the initial release density, release momentum, release direction (horizontal, vertical or at a certain angle), influence of crossflow by the combination of ambient currents and potential moving speed of the release structures, distance from the seabed, and the presence of the collector vehicle, should all be assessed and taken into account when significant influence on plume mixing and travel distance is expected. When local influences close to the equipment are important, different plume models are required for far-field plume dispersion and for near-field details of the release. Both the far-field and near-field will have their own appropriate level of detail and length/timescales involved, and it may not be feasible to combine both fields into one model. The near-field considers the zone of typically a few hundred meters where the plume behaves dynamically and local influences from equipment are important. This zone is likely to be smaller for DSM applications, as the mining vehicle and current speeds are lower than in dredging applications.

4.2 Overflow Plume (Far Field)

Far field considers the zone beyond the near field where the plume behaves passively being influenced by ambient currents, bathymetry, settling, deposition and resuspension. Depending on the zone of influence the far field for a TSHD plume can extend for tens of kilometers round a dredging project site. For DSM of nodules, it is not known what the exact far-field plume area will be. In laboratory experiments in a water column simulator, flocculation characteristics were observed (Gillard et al., 2019). These characteristics were then implemented in a plume dispersion model which estimated a far-field plume extent in the range of 4–9 km distance from the source Our results in **Section 2** indicate a similar range in the more favorable discharge scenarios as do validated models of DSM of crusts on seamounts (Spearman et al., 2020).

For dredge plumes in estuary mouths variations of velocity direction and magnitude in the vertical must be taken into account for correct plume dispersion simulations. When DSM process water is planned to be released higher in the water column it is very important to have the vertical stratification and velocity distribution included in the plume modelling. It is possible that higher in the water column the ambient currents have completely different magnitudes and directions than near the seabed and a plume can stay hanging on a gradient in ambient density for instance induced by temperature or salinity gradients.

4.3 Lessons Learned From Dredging for Deep-Sea Mining

A resemblance between DSM plumes from a collector and TSHD dredge plumes is that they are generated by a moving device. Especially when simulating deposition layers and potential for

smothering it is important to consider the details of operations like the work sequence, moving device locations in time, pauses in production. Because when simulations would be simplified with stationary sediment sources especially the amount of deposition and potential smothering near the release location can be overestimated while at the same time plume concentrations and deposition at locations further away could be underestimated.

Near-bed dredge plumes can stay near the bed for a long time because of turbulence damping at the steep density gradient at the top of the suspended sediment layer and when the density difference is large enough start behaving as a density current (Kirichek et al., 2021). DSM plumes are released near the seabed and ambient currents are weak so they can form a density current as well. Such density current will flow down bathymetry slopes which can be significant in the deep sea and a numerical tool used for DSM plumes should be able to deal with density currents when the release concentrations are high enough for a density current. Such numerical tool should have sufficient near-bed resolution and also include numerical measures to prevent artificially mixing up such near-bed density layer by for instance appropriate turbulence damping functions (Violeau, et al., 2002) otherwise the density current would numerically be destroyed which leads to underestimation of travel distances, deposition amounts, near-bed concentrations and overestimation of sediment concentrations further away from the bed.

Sediment spill fractions will be different for different types of equipment and will be dependent on sediment composition and equipment handling and production rate. For a proper DSM plume assessment, the spill characteristics, spill magnitude and sediment composition should be determined by taking into account the details of the spill generating processes of the specific equipment being used. This has to be done for all process steps which can generate spill including potential release of tailings and process water. Examples from dredging industry can serve as an example for such methodology (Becker et al., 2015; Laboyrie and Kolman, 2018) and a modelling framework for dredge plume assessment can be found in (Lisi et al., 2019).

DSM can also learn much from the experience of, and measurement protocols which are routinely applied to, dredge plume measurements (VBKO, 2003; CEDA, 2015a, b; Laboyrie and Kolman, 2018). Proper choice in measurement devices, calibration, measurement location, moment in time (interval and duration) are paramount to obtain the right insights into plume behavior. Stationary monitoring locations can be used or moving ones, or a combination of both. It is advisable to conduct proper baseline monitoring to know the natural sediment dynamics in the system at hand. In this way the increases in suspended sediment concentration (SSC) arising from plumes can be put into the context of natural background variation in SSC. This has been highlighted as an important issue for DSM (Spearman et al., 2020). For improving DSM plume modelling and spill term assessment it is important to make a connection between the measured plumes and the spill generating operations.

For dredging projects often turbidity (or SSC) limits, i.e., agreed thresholds in measured turbidity/SSC which establish the points at which more detailed measurements should be taken or when dredging activities should cease, are used to manage the environmental aspects of the dredging project. These limits should be based on the local situation and ecosystem at hand or otherwise there is the risk of having not enough protection of the environmental system or having too strict limits which unnecessarily make a project (much) more expensive. In practice turbidity/SSC limits are sometimes simply copied from another project without assessing whether they make sense for this different situation. For the new DSM industry there is an opportunity to do things better in this perspective and some ideas for determining appropriate environmental limits can be found in (CEDA, 2020)).

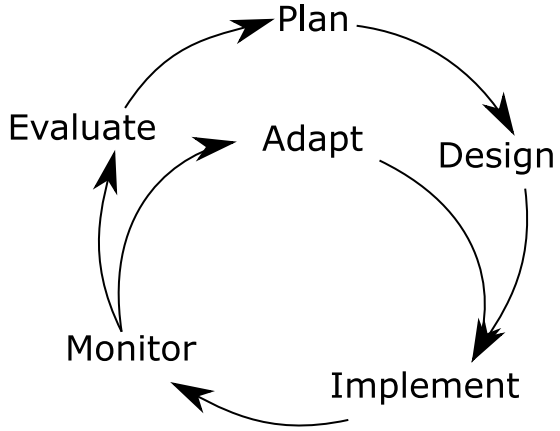

FIGURE 7 | Adaptive management cycle, adapted from (CEDA, 2015a, b) copyright CEDA.

4.4 The Adaptive Management Concept for Managing the Environmental Effects of Plumes

For some years, albeit not ubiquitously, the dredging industry has utilized a concept referred to as "adaptive management" to overcome the difficulties associated with production targets in an environment with (strict) environmental limits (CEDA, 2015a, b; Laboyrie and Kolman, 2018).

In (CEDA, 2015a, b) adaptive management is defined as decision framework that facilitates flexible decision-making that can be refined in response to future uncertainties, as outcomes from current and future management actions become better understood. **Figure 7** illustrates the adaptive management cycle. Adaptive management typically involves developing and implementing a management plan that defines the project goals, reviewing progress towards those goals periodically, and, in response to the outcomes of (environmental) monitoring, implementing corrective actions (and refining the plan), as needed, in future. Adaptive management is a formal process, with specifically agreed upon steps to deal with uncertainties. Adaptive management in

dredging projects prescribes a process wherein management actions can be changed in response to monitored system response, so as to maximise efficiency while maintaining or achieving a good ecological state. Adaptive management is suitable for those dredging projects where the outcome is less certain or accompanied by a low confidence in the prediction of effects. This applies to DSM as well and therefore adaptive management is a very useful decision framework for DSM.

5 SUMMARY AND CONCLUSIONS

Within this paper, we have addressed one of the environmental pressures that cause most concern for deep-sea mining, i.e., sediment plume dispersion. Before deep-sea mining can take place, it is of paramount importance that environmental pressures are investigated and measures are enacted to make sure that impacts are not too large. There is vast experience within the field of dredging engineering on how to manage and mitigate suspended sediment plumes. Although some of the characteristics of the processes might differ, there are many similarities in equipment and processes among dredging and deep-sea mining. Experience and best practices from the field of dredging engineering might be used to reduce, mitigate and manage suspended sediment plumes that would be generated by mining equipment. Our main findings are:

1. Based on the dimensional analysis presented in **Section 2**, the least plume dispersion for nodule DSM would be expected for slower mining vehicles. In that sense, for a comparable nodule production rate, it would be best to design the mining vehicle to be as wide as possible. That would then enable the collector to move forward more slowly, resulting in more favorable source conditions of the turbidity plume.
2. The suspended sediment plume is a direct result of the equipment-seabed interaction. Optimization of the mining equipment and processes are paramount to reduce the quantity of entrained water and/or sediment, and thus the source term of the sediment plume. Equal sediment fluxes are likely to disperse less when discharged at higher initial concentrations due to aggregation of particles.
3. In applications with production targets in an environment with (strict) environmental limits, adaptive management on environmental impact can be of assistance.
4. Various researchers have shown that the deep-sea sediment can aggregate, resulting in a net higher settling velocity. There are indications that flocculation processes in turbidity plumes can play a role in reducing its dispersion. However, at this stage, to what extent aggregation will occur in a dynamic flow is not well understood. It might well be that aggregation might be more profound for higher initial concentrations of a source term, as an additional effect to conclusion 2.

AUTHOR CONTRIBUTIONS

RH developed DSM context and near-field sediment plume characterization, both in dredging and DSM application. HdS carried out overview and contributions of relevant deep-sea sediment, especially at SMS and nodule deposits. LdW developed guidelines and shallow water near-bed plume interactions (dredging). JS provided dredging expertise, flocculation/particle aggregation and SMS/crusts modeling/experiments. RH coordinated and helped to draft the manuscript. All authors read and approved the final manuscript.

ACKNOWLEDGMENTS

RH and HS acknowledge funding from Blue Harvesting, EIT RM project 18138.

REFERENCES

Alvarez Grima, M., Miedema, S. A., Van de Ketterij, R. G., Yenigül, N. B., and Van Rhee, C. (2015). Effect of High Hyperbaric Pressure on Rock Cutting Process. *Eng. Geol.* 196, 24–36. doi:10.1016/j.enggeo.2015.06.016

Atkinson, J. (2017). *The Mechanics of Soils and Foundations*. London: Taylor & Francis.

Baas, J. H., Best, J. L., and Peakall, J. (2016). Comparing the Transitional Behaviour of Kaolinite and Bentonite Suspension Flows. *Earth Surf. Process. Landforms* 41, 1911–1921. doi:10.1002/esp.3959

Baker, E., and Beaudoin, Y. (2013). *Deep Sea Minerals: Sea-Floor Massive Sulphides, a Physical, Biological, Environmental and Technical Review*. Suva, Fiji: Secretariat of the Pacific Community and GRID-Arendal.

Baker, M. L., Baas, J. H., Malarkey, J., Jacinto, R. S., Craig, M. J., Kane, I. A., et al. (2017). The Effect of Clay Type on the Properties of Cohesive Sediment Gravity Flows and Their Deposits. *J. Sediment. Res.* 87, 1176–1195. doi:10.2110/jsr.2017.63

Becker, J., van Eekelen, E., van Wiechen, J., de Lange, W., Damsma, T., Smolders, T., et al. (2015). Estimating Source Terms for Far Field Dredge Plume Modelling. *J. Environ. Manag.* 149, 282–293. doi:10.1016/j.jenvman.2014.10.022

Bisschof, J., Heath, G., and Leinen, M. (1979). "Geochemistry of Deep-Sea Sediments from the Pacific Manganese Nodule Province DOMES Sites A, B and C," in *Marine Geology and Oceanography of the Pacific Manganese Nodule Province, Marine Science*. Editors J. Bisschof and D. Piper (Boston: Springer), 397–436.

Bleninger, T. (2000). *Sedimentation in Particle-Laden Jets*. Karlsruhe: University of Karlsruhe. PhD Dissertation.

Bonneaze, R., Huppert, H., and Lister, J. (1993). Particle-driven Gravity Currents. *J. fluid Mech.* 250, 339–369.

Boschen, R. E., Rowden, A. A., Clark, M. R., and Gardner, J. P. A. (2013). Mining of Deep-Sea Seafloor Massive Sulfides: A Review of the Deposits, Their Benthic Communities, Impacts from Mining, Regulatory Frameworks and Management Strategies. *Ocean Coast. Manag.* 84, 54–67. doi:10.1016/j.ocecoaman.2013.07.005

Bray, R. (2008). *Environmental Aspects of Dredging*. London: Taylor & Francis /Balkema.

CEDA (2020). *Assessing and Evaluating Environmental Turbidity Limits for Dredging*. Information paper. Retrieved from http://www.dredging.org/media/ceda/org/documents/resources/cedaonline/2020-05-AETL.pdf (Accessed March 7, 2022).

CEDA (2015a). *Environmental Monitoring Procedures*. Information paper. Retrieved from http://www.dredging.org/media/ceda/org/documents/resources/cedaonline/

2015-02-ceda_informationpaper-environmental_monitoring_procedures.pdf. (Accessed March 7, 2022).

CEDA (2015b). *Integratin Adaptive Environmental Management into Dredging Ports*. Position paper. CEDA. Retrieved from http://www.dredging.org/media/ceda/org/documents/resources/cedaonline/2015-01-ceda_positionpaper-integrating_adaptive_environmental_management_into_dredging_projects.pdf (Accessed March 7, 2022).

Cuthbertson, A. J. S., Apsley, D. D., Davies, P. A., Lipari, G., and Stansby, P. K. (2008). Deposition from Particle-Laden, Plane, Turbulent, Buoyant Jets. *J. Hydraul. Eng.* 134, 1110–1122. doi:10.1061/(asce)0733-9429(2008)134:8(1110)

de Wit, L. (2015). *3D CFD Modelling of Overflow Dredging Plumes*. Delft: Delft University of Technology. PhD. Dissertation.

de Wit, L., Talmon, A. M., and van Rhee, C. (2014a). 3D CFD Simulations of Trailing Suction Hopper Dredger Plume Mixing: A Parameter Study of Near-Field Conditions Influencing the Suspended Sediment Source Flux. *Mar. Pollut. Bull.* 88, 47–61. doi:10.1016/j.marpolbul.2014.08.043

de Wit, L., Talmon, A. M., and van Rhee, C. (2014b). 3D CFD Simulations of Trailing Suction Hopper Dredger Plume Mixing: Comparison with Field Measurements. *Mar. Pollut. Bull.* 88, 34–46. doi:10.1016/j.marpolbul.2014.08.042

Decrop, B., and De Wachter, T. (2019). "Detailed CFD Simulations for Near-Field Dispersion of Deep Sea Mining Plumes," WODCON XXII in 22nd World Dredging Conference, Shanghai, China, 116–127.

Decrop, B. (2015). *Numerical and Experimental Modelling of Near Field Overflow Dredging Plumes*. Ghent: Ghent University /KU Leuven. PhD Dissertation.

den Burger, M. (2003). *Mixture Forming Processes in Dredge Cutter Heads*. Delft: Delft University of Technology. PhD Dissertation.

Drazen, J. C., Smith, C. R., Gjerde, K. M., Haddock, S. H. D., Carter, G. S., Choy, C. A., et al. (2020). Opinion: Midwater Ecosystems Must Be Considered when Evaluating Environmental Risks of Deep-Sea Mining. *Proc. Natl. Acad. Sci. U.S.A.* 117, 17455–17460. doi:10.1073/pnas.2011914117

Erftemeijer, P., Riegl, B., Hoeksema, B. W., and Todd, P. A. (2012). Environmental Impacts of Dredging and Other Sediment Disturbances on Corals: A Review. *Mar. Pollut. Bull.* 64, 1737–1765. doi:10.1016/j.marpolbul.2012.05.008

Fettweis, M., and Baeye, M. (2015). Seasonal Variation in Concentration, Size, and Settling Velocity of Muddy Marine Flocs in the Benthic Boundary Layer. *J. Geophys. Res. Oceans* 120, 5648–5667. doi:10.1002/2014jc010644

Fischer, H., List, E., Koh, R., Imberger, J., and Brooks, N. (1979). *Mixing in Inland and Coastal Waters*. London: Academic Press.

Gerkema, T., Staquet, C., and Bouret-Aubertot, P. (2006). Decay of Semi-diurnal Internal-Tide Beams Due to Subharmonic Resonance. *Geophys. Res. Lett.* 33, L08604. doi:10.1029/2005gl025105

Gillard, B., Purkiani, K., Chatzievangelou, D., Vink, A., Iversen, M., and Thomsen, L. (2019). Physical and Hydrodynamic Properties of Deep Sea Mining-Generated, Abyssal Sediment Plumes in the Clarion Clipperton Fracture Zone (Eastern-central Pacific). *Elem. Sci. Anthropocene* 7. doi:10.1525/elementa.343

Gladstone, C., Phillips, J., and Sparks, P. (1998). Experiments on Bidisperse, Constant-volume Gravity Currents: Propagation and Sediment Deposition. *Sedimentology* 45, 833–843. doi:10.1046/j.1365-3091.1998.00189.x

Global Sea Mineral Resources NV (2018). *Environmental Impact Statement: Small-Scale Testing of Nodule Collector Components on the Seafloor of the Clarion-Clipperton Fracture Zone and its Environmental Impact*. Retrieved from https://www.isa.org.jm/files/files/documents/GSR-EIS-compact.zip (Accessed March 7, 2022).

Gollner, S., Kaiser, S., Menzel, L., Jones, D. O. B., Brown, A., Mestre, N. C., et al. (2017). Resilience of Benthic Deep-Sea Fauna to Mining Activities. *Mar. Environ. Res.* 129, 76–101. doi:10.1016/j.marenvres.2017.04.010

Hein, J., and Koschinsky, A. (2014). "Deep Ocean Ferromanganese Crusts and Nodules," in *Treatise in Geochemistry*. Editors H. Holland and K. Turekian. second edition (Elsevier), Vol. 13. chapter 11. doi:10.1016/b978-0-08-095975-7.01111-6

Hein, J., and Petersen, S. (2013). *The Geology of Cobalt-Rich Ferromanganese Crusts*. Noumea: SPC.

Hein, J. R., Koschinsky, A., and Kuhn, T. (2020). Deep-ocean Polymetallic Nodules as a Resource for Critical Materials. *Nat. Rev. Earth Environ.* 1 (3), 158–169. doi:10.1038/s43017-020-0027-0

Helmons, R., Elerian, M., Bedon Vasquez, A., and de Stigter, H. (2019). "Sediment Discharges from Mining Vehicles, Experiments to Fin the Optimal Release Conditions," in 49th Underwater Maining Conference, Sanya, China.

Helmons, R. L. J., Miedema, S. A., Alvarez Grima, M., and Van Rhee, C. (2016). Modeling Fluid Pressure Effects when Cutting Saturated Rock. *Eng. Geol.* 211, 50–60. doi:10.1016/j.enggeo.2016.06.019

Jirka, G. H. (2007). Buoyant Surface Discharges into Water Bodies. II: Jet Integral Model. *J. Hydraul. Eng.* 133, 1021–1036. doi:10.1061/(asce)0733-9429(2007)133:9(1021)

JOGMEC. (2020). JOGMEC Conducts Worlds First Successful Excavation of Cobalt-Rich Seabed in the Deep Ocean. Retrieved from http://www.jogmec.go.jp/english/news/release/content/300368332.pdf (Accessed March 7, 2022).

Jones, D. O. B., Kaiser, S., Sweetman, A. K., Smith, C. R., Menot, L., Vink, A., et al. (2017). Biological Responses to Disturbance from Simulated Deep-Sea Polymetallic Nodule Mining. *PLoS One* 12, e0171750. doi:10.1371/journal.pone.0171750

Jones, D. O. B., Simon-Lledó, E., Amon, D. J., Bett, B. J., Caulle, C., Clément, L., et al. (2021). Environment, Ecology, and Potential Effectiveness of an Area Protected from Deep-Sea Mining (Clarion Clipperton Zone, Abyssal Pacific). *Prog. Oceanogr.* 197, 102653. doi:10.1016/j.pocean.2021.102653

Kaiser, S., Smith, C. R., and Arbizu, P. M. (2017). Editorial: Biodiversity of the Clarion Clipperton Fracture Zone. *Mar. Biodiv.* 47, 259–264. doi:10.1007/s12526-017-0733-0

Kirichek, A., Cronin, K., de Wit, L., and van Kessel, T. (2021). "Advances in Maintenance of Ports and Waterways: Water Injection Dredging," in *Sediment Transport - Recent Advances*.

Kooistra, A., Verhoef, P., Broere, W., Ngan-Tillard, D., and Tol, A. (1998). "Appraisal of Stickiness of Natural Clays from Laboratory Tests," in *Publications of the Applied Earth Sciences, Section Engineered Geology*.

Laboyrie, V., and Kolman, R. (2018). *Dredging for Sustainable Infrastructure*. Revision no. 673. Voorburg: CEDA /IADC.

Lang, A., Dasselaar, S., Aasly, K., and Larsen, E. (2019). Blue Nodules Deliverable Report D3.4: Report Describing the Process Flow Overview.

Lavelle, J. W., and Mohn, C. (2010). Motion, Commotion, and Biophysical Connections at Deep Ocean Seamounts. *Oceanog.* 23, 90–103. doi:10.5670/oceanog.2010.64

Lee, W. Y., Li, A. C. Y., and Lee, J. H. W. (2013). Structure of a Horizontal Sediment-Laden Momentum Jet. *J. Hydraul. Eng.* 139, 124–140. doi:10.1061/(asce)hy.1943-7900.0000662

Lenoble, J. (2000). *Overview of the Authority's Regulations and Recommendations to Ensure the Effective Protection of the Marine Environment from Harmful Effects that May Arise from Activities in the Area*. Kingston, Jamaica: International Seabed Authority.

Lisi, I., Feola, A., Bruschi, A., Pedroncini, A., Pasquali, D., and Di Risio, M. (2019). Mathematical Modeling Framework of Physical Effects Induced by Sediments Handling Operations in Marine and Coastal Areas. *J. Mar. Sci. Eng.* 7 (5), 149.

Liu, P., and Lam, K. M. (2013). Two-phase Velocity Measurement in a Particle-Laden Jet. *J. Hydro-Environ. Res.* 7, 18–29. doi:10.1016/j.jher.2012.08.001

Manning, A. J., and Dyer, K. R. (2007). Mass Settling Flux of Fine Sediments in Northern European Estuaries: Measurements and Predictions. *Mar. Geol.* 245, 107–122. doi:10.1016/j.margeo.2007.07.005

Marr, J. G., Harff, P. A., Shanmugam, G., and Parker, G. (2001). Experiments on Subaqueous Sandy Gravity Flows: The Role of Clay and Water Content in Flow Dynamics and Depositional Structures. *Bull. Geol. Soc. Am.* 113, 1377–1386. doi:10.1130/0016-7606(2001)113<1377:eossgf>2.0.co;2

Munoz-Royo, C., Peacock, T., Alford, M., Smith, J., Le Boyer, A., Kulkarni, C., et al. (2021). Extent of Impact of Deep-Sea Nodule Mining Midwater Plumes Is Influenced by Sediment Loading, Turbulence and Thresholds. *Commun. Earth Environ.* 2 (1), 1–16. doi:10.1038/s43247-021-00213-8

Nauru Ocean Resources Inc (2021). *Collector Test Study: Environmenta Impact Statement*. Nauru Ocean Resources Inc.

Nautilus Minerals (2008). *Environmental Impact Statement, Nautilus Mineral Niugini Limited, Solwara 1 Projects, Volume B, Appendix 12, Modelling the Dispersion of Returned Water Discharge Plume from the Solwara 1 Seabed Mining Project*. Manus Basin, Papua New Guinea: Nautilus Minerals.

Neves, M., Neves, A., and Bleninger, T. (2002). "Prediction on Particle Deposition in Effluent Disposal System," in Proceeding 2nd International Conference On Marine Waste Water Discharges.

Nichols, M., Diaz, R. J., and Schaffner, L. C. (1990). Effects of Hopper Dredging and Sediment Dispersion, Chesapeake Bay. *Environ. Geol. Water Sci.* 15, 31–43. doi:10.1007/bf01704879

Oebius, H. U., Becker, H. J., Rolinski, S., and Jankowski, J. A. (2001). Parametrization and Evaluation of Marine Environmental Impacts Produced by Deep-Sea Manganese Nodule Mining. *Deep Sea Res. Part II Top. Stud. Oceanogr.* 48, 3453–3467. doi:10.1016/s0967-0645(01)00052-2

Okamoto, N., Shiokawa, S., Kawano, S., Yamaji, N., Sakurai, H., and Kurihara, M. (2019). "World's First Lifting Test for Seafloor Massive Sulphides in the Okinawa Trough in the EEZ of Japan," in The 29th International Ocean and Polar Engineering Conference (Honolulu, Hawaii, USA: ISOPE), ISOPE-1-19-655.

Ouillon, R., Kakoutas, C., Meiburg, E., and Peacock, T. (2021). Gravity Currents from Moving Sources. *J. Fluid Mech.* 924, A43. doi:10.1017/jfm.2021.654

Pagliai, A., Varriale, A., Crema, R., Galletti, M., and Zunarelli, R. (1985). Environmental Impact of Extensive Dredging in a Coastal Marine Area. *Mar. Pollut. Bull.* 16, 483–488. doi:10.1016/0025-326x(85)90381-9

Ramirez-Llodra, E., Tyler, P. A., Baker, M. C., Bergstad, O. A., Clark, M. R., Escobar, E., et al. (2011). Man and the Last Great Wilderness: Human Impact on the Deep Sea. *PLoS One* 6, e22588. doi:10.1371/journal.pone.0022588

Smith, S. J., and Friedrichs, C. T. (2011). Size and Settling Velocities of Cohesive Flocs and Suspended Sediment Aggregates in a Trailing Suction Hopper Dredge Plume. *Cont. Shelf Res.* 31, S50–S63. doi:10.1016/j.csr.2010.04.002

Spagnoli, G., Freudenthal, T., Strasser, M., and Weixler, L. (2014). "Development and Possible Applications of Mebo200 for Geotechnical Investigations for the Underwater Mining," in Offshore Technology Conferene, Houston, Texas, USA, OTC-25081.

Spearman, J., De Heer, A., Aarninkhof, S., and Van Koningsveld, M. (2011). Validation of the TASS System for Predicting the Environmental Effects of Trailing Suction Hopper Dredging. *Terra Aqua* 125, 14.

Spearman, J. (2014). Prediction of the Overflow of Sediment from Trailing Dredgers. *Marit. Eng.* 167, 82–96. doi:10.1680/maen.13.00019

Spearman, J., Taylor, J., Crossouard, N., Cooper, A., Turnbull, M., Manning, A., et al. (2020). Measurement and Modelling of Deep Sea Sediment Plumes and Implications for Deep Sea Mining. *Sci. Rep.* 10, 5075. doi:10.1038/s41598-020-61837-y

Ungarish, M. (2009). *An Introduction to Gravity Currents and Intrusions*. New York, NY: CRC Press.

van Grunsven, F., Keetels, G., and van Rhee, C. (2018). "The Initial Spreading of Turbidity Plumes - Dedicated Laboratory Experiments for Model Validation," in 48th Underwater Mining Conference (UMC) 2018, Bergen, Norway.

van Haren, H. (2018). Abyssal Plain Hills and Internal Wave Turbulence. *Biogeosciences* 15, 4387–4403. doi:10.5194/bg-15-4387-2018

van Haren, H., and Gostiaux, L. (2012). Energy Release through Internal Wave Breaking. *oceanog* 25, 124–131. doi:10.5670/oceanog.2012.47

van Haren, H., Hanz, U., de Stigter, H., Mienis, F., and Duineveld, G. (2017). Internal Wave Turbulence at a Biologically Rich Mid-Atlantic Seamount. *PLoS ONE* 12, e0189720. doi:10.1371/journal.pone.0189720

van Haren, H., Maas, L. R. M., and Gerkema, T. (2010). Patchiness in Internal Tidal Beams. *J. Mar. Res.* 68, 237–257. doi:10.1357/002224010793721451

van Rhee, C. (2002). *On the Sedimentation Process in a Trailing Suction Hopper Dredger*. Delft: Delft University of Technology. PhD Dissertation.

van Wijk, J. M., Haalboom, S., de Hoog, E., de Stigter, H., and Smit, M. G. (2019). Impact Fragmentation of Polymetallic Nodules under Deep Ocean Pressure Conditions. *Miner. Eng.* 134, 250–260. doi:10.1016/j.mineng.2019.02.015

VBKO (2003). *Protocol for the Field Measurement of Sediment Release from Dredgers*. The Hague: VBKO TASS project.Issue I.

Violeau, D., Bourban, S., Cheviet, C., Markofsky, M., Petersen, O., Roberts, W., et al. (2002). "Numerical Simulation of Cohesive Sediment Transport : Intercomparison of Several Numerical Models," in *Fine Sediment Dynamics in the Marine Environment*. Editors J. Winterwerp and C. Kranenburg (Elsevier), 75–89. doi:10.1016/s1568-2692(02)80009-2

Volz, J. B., Mogollón, J. M., Geibert, W., Arbizu, P. M., Koschinsky, A., and Kasten, S. (2018). Natural Spatial Variability of Depositional Conditions, Biogeochemical Processes and Element Fluxes in Sediments of the Eastern Clarion-Clipperton Zone, Pacific Ocean. *Deep Sea Res. Part I Oceanogr. Res. Pap.* 140, 159–172. doi:10.1016/j.dsr.2018.08.006

Washburn, T. W., Turner, P. J., Durden, J. M., Jones, D. O. B., Weaver, P., and Van Dover, C. L. (2019). Ecological Risk Assessment for Deep-Sea Mining. *Ocean Coast. Manag.* 176, 24–39. doi:10.1016/j.ocecoaman.2019.04.014

Wedding, L. M., Reiter, S. M., Smith, C. R., Gjerde, K. M., Kittinger, J. N., Friedlander, A. M., et al. (2015). Managing Mining of the Deep Seabed. *Science* 349, 144–145. doi:10.1126/science.aac6647

Winterwerp, J. C. (2002). Near-field Behavior of Dredging Spill in Shallow Water. *J. Waterw. Port. Coast. Ocean. Eng.* 128, 96–98. doi:10.1061/(asce)0733-950x(2002)128:2(96)

Yamazaki, T., Cung, J., and Tsurusaki, K. (1995). Geotechnical Parameters and Distribution Characteristics of the Cobalt-Rich Manganese Crust for the Mining Design. *Int. J. Offshore Polar Eng.* 5 (01), 75–79.

Yong, R., Nakano, M., and Pusch, R. (2012). "Nature of Soils," in *Environmental Soil Properties and Behavior*, 133–161.

Zawadzki, D., Maciąg, Ł., Abramowski, T., and McCartney, K. (2020). Fractionation Trends and Variability of Rare Earth Elements and Selected Critical Metals in Pelagic Sediment from Abyssal Basin of NE Pacific (Clarion-Clipperton Fracture Zone). *Minerals* 10, 320. doi:10.3390/min10040320

Conflict of Interest: Author JS was employed by the company HR Wallingford, Dredging and Coasts & Oceans.

The remaining authors declare that the research was conducted in the absence of any commercial or financial relationships that could be construed as a potential conflict of interest.

Publisher's Note: All claims expressed in this article are solely those of the authors and do not necessarily represent those of their affiliated organizations, or those of the publisher, the editors and the reviewers. Any product that may be evaluated in this article, or claim that may be made by its manufacturer, is not guaranteed or endorsed by the publisher.